Published in final edited form as:
Anticancer Res. 2011 April ; 31(4): 1093–1103.

Synergistic Activity of Histone Deacetylase and Proteasome Inhibition Against Pancreatic and Hepatocellular Cancer Cell Lines

J.L. Spratlin[1,3], **T.M. Pitts**[1], **G.N. Kulikowski**[1], **M.P. Morelli**[1], **J.J. Tentler**[1], **N.J. Serkova**[2], and **S.G. Eckhardt**[1]

[1]Division of Medical Oncology, School of Medicine, University of Colorado Anschutz Medical Campus, Aurora, CO, U.S.A

[2]Department of Anesthesiology, Animal Imaging Cancer Center Core, School of Medicine, University of Colorado at Denver, Aurora, CO, U.S.A

[3]Department of Medicine, Cross Cancer Institute, University of Alberta, Edmonton, Alberta, Canada

Abstract

Aim—To determine the phenotypic effects of belinostat (bel) and bortezomib (bor) against pancreatic cancer (PC) and hepatocellular cancer (HCC) cell lines.

Materials and Methods—Antiproliferative effects were assessed using a sulforhodamine B assay. Synergy was evaluated using the Chou and Talalay method. Apoptosis was measured by caspase −31 −7 activity and PARP cleavage. Downstream effector proteins were detected via immunoblotting. Quantitative nuclear magnetic resonance (NMR)-based metabolomics analysis was performed.

Results—There were single-agent antiproliferative effects against PC and HCC cell lines; the combination of bel and bor (bel+bor) had a synergistic effect. There was up to a 45-fold induction of apoptosis over the control. Post-treatment cell death was associated with p21 up-regulation, more pronounced with treatment with bel+bor. Treatment with bel+bor enhanced hyperacetylation of histone H3 over single-agent bel. A metabolic signature was established for treatments with bor and bel+bor.

Conclusion—The combination of bel+bor displayed significant antiproliferative activity against PC and HCC cell lines, with exhibiting synergistic antiproliferative and proapoptotic patterns even at suboptimal single-agent doses.

Keywords

Belinostat; bortezomib; pancreas cancer; histone deacetylase inhibitor; proteasome inhibitor; hepatocellular cancer; apoptosis; metabolomics

Pancreatic cancer (PC) is the fourth leading cause of cancer death in the U.S.A. with the yearly incidence approaching the yearly death rate (1). Survival after diagnosis of PC is dismal with less than 5% of patients achieving cure. Attempts at palliative chemotherapy

Correspondence to: Assistant Professor Jennifer L. Spratlin, MD FRCPC, Medical Oncology, Cross Cancer Institute, University of Alberta, 11560 University Avenue, Edmonton, Alberta, Canada, T6G. Tel: +1 7804328513, Fax: +1 7804328888, jennifer.spratlin@albertahealthservices.ca.

have yielded limited efficacy. The nucleoside analogue gemcitabine is considered the standard of care treatment, although less than one fourth of patients experience clinical benefit with only a 1.24 month improvement in median survival when gemcitabine is compared to 5-fluorouracil. Additionally, only a 0.34 month benefit in median survival is achieved when a biologic agent is added to gemcitabine (2, 3).

Hepatocellular carcinoma (HCC) is one of the most prevalent types of cancer worldwide. There is a rising incidence of HCC in the U.S.A., likely related to the increase in the diagnosis of hepatitis C. Curative surgical resection is possible for patients diagnosed with localized disease; however this option is limited to a small number of patients with good performance status, adequate liver function and a small burden of disease in an anatomic location amenable to surgical removal of all tumor(s). For all other patients, limited local ablative treatments and systemic therapies exist. Furthermore, no standard chemotherapeutic regimen has demonstrated a survival benefit over best supportive care (BSC) in HCC. Sorafenib, a multi-targeted tyrosine kinase inhibitor, has recently filled the systemic treatment void in advanced disease with reports of improvement in overall survival over BSC with a tolerable toxicity profile. However, the benefit in overall survival was just 2.8 months with the caveat that patients enrolled on this study had Child Pugh A status (4). Clearly, there is a need for new therapeutic agents and strategies for these malignancies.

Belinostat (bel), (PXD101; Curagen, New Haven, CT, USA) is a histone deacetylase (HDAC) inhibitor. Histones are a highly conserved group of proteins whose function is to compact deoxyribonucleic acid (DNA), thereby altering its structure and modifications, resulting in altered gene transcription (5). Modifications of histones occur primarily through post-translational acetylation of lysine residues. The acetylation status of histones is regulated by a balance in the activity of histone acetyl transferases (HATs) and HDACs, which add and remove acetyl groups from histones, respectively. The acetylation status of histones regulates gene transcription by allowing access of transcriptional machinery to portions of DNA when histones are acetylated, thereby promoting a more relaxed chromatin structure, or by disallowing access and inhibiting transcription when histones are deacetylated, thereby promoting chromatin condensation.

Four classes of HDACs exist, with enzyme overexpression noted in many cancer types including colon, gastric, prostate and breast cancer (6). Preclinically, HDACs mediate the functions of oncogenes, improper function of HDAC results in tumor formation and HDAC mutations have been linked to aberrant cellular growth and tumor proliferation (7–10). Data have shown that inhibition of HDACs activates multiple antineoplastic pathways, including induction of growth arrest and activation of proapoptotic pathways, as well as promotion of cell death caused through mitotic, autophagic and free-radical pathways (reviewed in (11)). Currently, vorinostat (Merck, NJ, USA) is the only approved HDAC inhibitor for anticancer therapy with approval for cutaneous manifestations of cutaneous T-cell lymphoma (12). Notably however, many other HDAC inhibitors are undergoing assessment in phase I, II and III clinical trials (13). Bel, a class I and II HDAC inhibitor, inhibits the proliferation of cancer cell lines at low micromolar potencies and is currently being evaluated as single agent and in combination with other treatments in multiple phase I and II clinical trials (14–19).

Bortezomib (bor) is a potent inhibitor of the 26S proteasome, a multicatalytic enzyme complex that degrades intracellular proteins by a controlled mechanism targeting the ubiquitin pathway. The proteasomal protein disposal pathway is essential in the degradation of proteins mediating multiple cellular processes, including cell-cycle regulation, apoptosis, transcription, stress response, DNA repair and cellular differentiation (20, 21). Although the exact mechanisms of protein degradation within the proteasome are not presently

understood, proper functioning of this system is essential for normal cellular function and for the recycling and reuse of individual amino acids and oligopeptides. Inhibition of the proteasome causes a decrease in proliferation and migration and induction of apoptosis through multiple mechanisms most commonly *via* down-regulation of nuclear factor-kappa B (NFκB) (20). Alternate proapoptotic pathways include stabilization of p53, Bid, Bax, p21, p27, caveolin-1, or up-regulation of JNKb (22). Bor is currently approved for use as an anticancer agent for second- and third-line use in multiple myeloma, second-line mantle cell lymphoma and is being investigated in phase II studies in various solid tumors

The pathophysiology of both PC and HCC is not fully elucidated. It is likely that the mechanisms of carcinogenesis, proliferation, promotion of metastases and induction of cancer cell death are distinct in each disease. Nonetheless, both PC and HCC have demonstrated resistance to traditional cytotoxic therapies and new approaches incorporating both novel agents and rational combinations are needed to overcome the current stalemate of repetitive negative clinical trial results. Based on previous results from this research group with combined HDAC and proteasome inhibition in colorectal cancer cell lines, this study evaluated the effects of bel and bor against human PC and HCC models, hypothesizing that the combination of HDAC and proteasome inhibition would induce synergistic inhibition of cell proliferation and induction of apoptosis, thereby providing a rationale for the clinical testing of this combination in these diseases. Therefore, single-agent and combination studies were conducted to evaluate the antiproliferative and proapoptotic effects of bel and bor, in addition to the assessment of downstream effectors by immunoblotting and metabolic responses using multi-nuclear magnetic resonance (NMR)-based metabolomics.

Materials and Methods

Cell lines, cell culture and drug supply

The PC and HCC cell lines, BxPC3 (*p53*-mutated, *ras* wild-type), Panc1 (*p53*-mutated, *ras*-mutated), Hep1 (*p53*-mutated, *ras* wild-type) and HepG2 (*p53* wild-type, *ras*-mutated) were obtained from the American Type Culture Collection (Manassas, VA, USA). Cells were grown in DMEM supplemented with 10% fetal bovine serum, 1% non-essential amino acids, 1% penicillin/streptomycin and were maintained at 37°C in an incubator under an atmosphere containing 5% CO_2. Cultures were routinely screened for mycoplasma (MycoAlert; Cambrex Bio Science, Baltimore, MD, USA) and were exposed to drugs when they reached approximately 70% confluence. Bel was provided through the Cancer Therapy Evaluation Program (CTEP), a National Cancer Institute program sponsoring clinical and pre-clinical investigations evaluating new cancer treatments. Bor was obtained from the University of Colorado Pharmacy and prepared as per the drug insert.

Evaluation of cytotoxicity and effects of drug combination

Cells were initially exposed to single agent bel or bor for 24, 48 and 72 h. Cytotoxic effects were determined using the sulforhodamine B (SRB) assay (23). Briefly, 100 μl of cell suspension containing 4,000 viable BxPC3, Panc1, Hep1 or HepG2 cells in logarithmic growth phase were plated in 96-well flat-bottom plates with lids and allowed to attach for 24 h. After incubation overnight, cells were exposed to increasing concentrations of bel (0–8 μM) or bor (0–100 nM), added to wells in 2× concentration in 100 μl of media. Media was then removed and cells fixed with cold 10% trichloroacetic acid for 30 min at 4°C, followed by cell washing with water and staining with 0.4% SRB for 30 min at room temperature. Cells were then washed again with 1 % acetic acid after which the SRB stain was solubilized with 10 mM Tris at room temperature. The plate was then read on a plate reader with the wavelength set at 565 or 490 nm. Cell proliferation curves were derived from the

raw optical density (OD) data to determine the single-agent 50% inhibitory concentration (IC_{50}), a measure of drug potency.

To determine potential antiproliferative synergy, bel and bor were tested in combination at three different concentrations of each drug based on the individual drug IC_{50} values, with the doses corresponding to the IC_{50}, one dose below and one dose above. Using these concentrations, all combinations of the drugs were assessed, with exposure durations of 24, 48 and 72 h. Cells were plated as per single-agent studies and proliferation was measured by the SRB assay. Results of the combination treatment were analyzed according to the isobolographic method of Chou and Talalay using the Calcusyn software program (Biosoft, Cambridge, UK) (24). A combination index (CI), measuring the degree of interaction between the two drugs was determined, where CI=1 denotes additivity; >1, antagonism; <1, synergism.

Induction of apoptosis

Four thousand viable BxPC3, Panc1, Hep1 or HepG2 cells were plated in 96-well, white-walled plates and allowed to attach for 24 h. Cells were then treated with single agent bel, bor, or bel plus bor at the same doses as those used for the antiproliferative assessments (Table I) for 24, 48 and 72 h, after which apoptosis was determined *via* luminometric Caspase-Glo 3/7 assay (Promega, La Jolla, CA, USA) according to the manufacturer's protocol, using a Synergy 2 plate reader (BioTek, Winooski, VT, USA). Cellular apoptosis was expressed as a fold-increase over untreated control cells.

Apoptosis and immunoblotting

A time course to investigate the proapoptotic synergy and immunoblotting for biomarkers of drug effect was undertaken at 4, 8, 12, 16 and 24 h of single-agent or combination drug exposure. Cells were plated, exposed to single agent or the combination of drugs and the Caspase-Glo 3/7 assay was performed as described above at these time points. For simplicity, with this time course, bel and bor doses were standard across all cell lines with exposure doses being 0.5, 1 and 2 μM and 10, 20 and 40 nM, respectively. Immunoblotting for total poly (ADP-ribose) polymerase (tPARP), acetylated histone 3 (aH3), p21, and phosphorylated NFκB (p-NFκB) were completed at the same time points, but using only the two lowest doses of bel and bor used in the apoptosis time course (0.5 μM and 1 μM;10 nM and 20 nM, respectively). Briefly, cells were seeded into 6-well plates, left to attach for 24 h and then treated with single-agent bel or bor, or all permutations of the combination of drugs. After drug exposure, cells were scraped into RIPA buffer containing protease inhibitors, EDTA, NaF and sodium orthovanadate. The total protein in samples was determined *via* BioRad Dc Protein Assay (BioRad, Hercules, CA, USA). An amount of 40 μg total protein was loaded onto a 10% polyacrylamide gel, electrophoresed and then transferred to polyvinylidene fluoride (PVDF) membranes using the iBLOTtransfer system (Invitrogen, Carlsbad, CA, USA). Membranes were blocked for 1 h at room temperature with 5% non-fat dry milk in TBS-containing tween-20 (0.1%) and then incubated overnight at 4°C with one of the following primary antibodies (all from Cell Signaling, Beverly, MA, USA): anti-p21 mouse monoclonal antibody at 1:5,000, anti-total PARP antibody at 1:5,000, anti-acetylated histone 3 antibody at 1:5000 and anti-p-NFκB antibody at 1:1,000. Membranes were then washed three times for 20 min in TBS-Tween (0.1%) and then incubated for 1 h with the appropriate secondary anti-mouse or anti-goat IgG horseradish peroxidase-linked antibody at 1:20,000 (Jackson ImmunoResearch, West Grove, PA, USA). Three additional washes with TBS-Tween (0.1%) preceded membrane development by Immobilon Western Chemiluminescent HRP substrate (Millipore, Billerica, MA, USA).

Quantitative NMR-based metabolomics

For metabolic response assessment, one PC (BxPC3) and one HCC (Hep1) cell line, both ras wild-type, were treated with bel (500 nM) and bor (20 nM), the lowest concentrations used in the apoptosis assays, or bel and bor for 24 and 48 h. Untreated control cells were exposed to the vehicle (DMSO) at its highest concentrations in the combination group. The last four hours of incubation, [1–^{13}C] glucose containing medium (5 mM) was used in order to assess glucose uptake and metabolism in treated cells. After drug treatment, the cells were washed and extracted with 12% perchloric acid (to precipitate proteins and macromolecules), as described previously (25–27). After the hydrophilic fractions were collected and ^{13}C-media were freeze-dried overnight, the extracts were re-dissolved in deuterium oxide (D_2O, 0.5 and 1 ml for cell and medium extracts, respectively). The dissolved extracts then underwent 1H-, ^{13}C- and ^{31}P-NMR spectroscopy for a quantitative analysis of cell endogenous metabolites and metabolite fluxes (cell extracts) as well as of substrate uptake and export (medium extracts).

High-resolution ^{1}H- and ^{13}C-NMR experiments were performed with the Bruker 500 MHz DRX spectrometer equipped with an inverse 5-mm TXI probe (BrukerBioSpin, Fremont, CA, USA), while ^{31}P-NMR experiments were performed with the 300MHz Bruker Avance system with a 5-mm QNP probe (26, 27). Trimethylsilyl propionic-2,2,3,3,-d_4 acid (TSP, 0.5 mmol/1) was used as an external standard for metabolite chemical shift assignment (0 ppm) and quantification (for exact metabolite assignment and their chemical shifts refer to (28)). Methylenediphosphoric acid (2 mmol/1) was used as an external standard for chemical shift references (18.6 ppm) and for metabolite quantification in ^{31}P-NMR. For calculation of ^{13}C-enrichment of glucose and glucose metabolites, [3–^{13}C] lactate satellite peak (at 1.23 ppm) from ^{1}H-NMR spectra served as an internal standard for ^{13}C-NMR spectra (at 21 ppm) (27). All data were processed using the Bruker WINNMR program. All NMR experiments were performed at the Metabolomics NMR University of Colorado Cancer Center Core.

For each NMR treatment group, four replicates were performed (n=4). All numerical data are presented as mean±standard deviation from the replicate experiments. One-way analysis of variance (ANOVA) was used to determine differences between groups. Tukey's test was used as a *post-hoc* test in combination with ANOVA to test for significances between groups. The significance level was set at $p<0.05$ for all tests. Statistical analyses was performed using the programs SigmaPlot version 9.01 (Systat Software, Point Richmond, CA, USA) and SPSS version 14.0 (SPSS Inc., Chicago, IL, USA).

Results

Synergistic antiproliferative effects of belinostat and bortezomib

PC and HCC cell lines were exposed to bel and bor as single agents and the antiproliferative IC_{50} values for each cell line, as a function of exposure duration, are listed in Table I. Interestingly, an IC_{50} value was not achievable in any cell line after 24 h of bel exposure, whereas exposure to bor resulted in IC_{50} values of 100 and 50 nM against the BxPC3 and Hep1 cells, respectively. Clearly, there was a trend towards greater potency of bel effects at 48 and 72 h against all but the HepG2 cells, while bor effects remained fairly stable with less than a fold-change between these two time points.

The combination of bel and bor was assessed for synergy and a consistent synergistic inhibition of proliferation was demonstrated across all cell lines and time points as demonstrated by CI values of less than 1 (data not shown). As an example, as shown in Figure 1A–C, the range of CI results for the Panc1 cell line was 0.17–0.47, 0.22–0.55 and 0.18–0.65 at 24, 48 and 72 h, respectively. Importantly, synergy was observed at

concentrations less than the single-agent IC_{50} values, indicating true potentiation of the growth inhibitory effects by the combination. As further evidence for this, the CI values were the lowest (greatest synergy) in all cell lines except BxPC3 at 24 h, a time point at which an IC_{50} value was not obtained for bel against any cell line.

Induction of apoptosis with the combination of bel and bor

To determine whether the observed synergy was associated with induction of cell death, the ability of bel and bor to induce apoptosis was assessed, individually and in combination, by measuring the activity of caspase−3/−7 after drug exposure for 24, 48 and 72 h. The single agents resulted in only a modest increase in apoptosis that was more pronounced with bor compared to bel. When the drugs were used in combination, the increase in apoptosis compared to controls was dramatic, reaching up to 13-, 16-, 11- and 38-fold for the BxPC3, Panc1, Hep1, and HepG2 cell lines, respectively. The greatest induction of apoptosis with bel plus bor was observed at 24 h, with minimal increases observed at 72 h across all cell lines.

In light of these findings, an early treatment time course was performed to ascertain whether maximum apoptosis was occurring earlier than 24 h. In all cell lines, peak apoptosis occurred at 12 h of drug exposure with the greatest induction occurring in the combination groups. For example, the HepG2 cell line demonstrated the greatest induction of apoptosis with over a 40-fold increase observed in some combination concentrations, as depicted in Figure 2.

Downstream effectors of bel and bor therapy

To assess downstream effectors of each drug, immunoblotting was performed for: (i) p21, a marker of cell cycle arrest, (ii) aH3, which is acetylated by HDAC inhibition, (iii) PARP), an enzyme required for progress through the late stages of apoptosis which captures full length and cleaves PARP at 116 and 89 kDa, respectively and (iv) p-NFκB, which traditionally is down-regulated with bor exposure and is thought to mediate proteasome inhibition-associated apoptosis. Based on the mechanisms of action of each drug, it was hypothesized that the following observation would be made: (i) an increase in aH3 expression after bel, (ii) a decrease in p-NFκB expression after bor and (iii) an increase in p21 and cleaved PARP expression with bel+bor. Results for the BxPC3 and Hep1 cell lines at 12 h are depicted in Figure 3. As expected, increased aH3 was associated with bel exposure and was maintained on treatment with bel and bor combination. Surprisingly, p-NFκB was increased after the highest dose of bel and both doses of bor; this effect was additive in combination therapy. This effect was more pronounced in the Hep1 compared to the BxPC3 cells. As expected, based on the antiproliferative and proapoptotic data, the cell-cycle arrest protein p21 increased after bel and bor exposure and appeared to further increase with combination treatment. This up-regulation was more pronounced in the PC compared to HCC cell lines. Lastly, as a confirmatory marker of proapoptotic effects, the degree of PARP cleavage was evaluated. Although both bel and bor led to some cleaved PARP product, there was near complete cleavage in all combinations, which was more pronounced in the BxPC3 cells.

Metabolomic responses to bel, bor and their combination

For each experiment a total of 51 metabolic endpoints were assessed using a multinuclear NMR approach. The absolute concentrations of 43 metabolites and 8 metabolite ratios are depicted in Figure 4. Glucose uptake and lactate export were calculated from media extracts, whereas the intracellular concentrations of various metabolites (including ^{13}C-labeled intermediates from glucose metabolites) and their ratios were calculated from NMR spectra of cell extracts. Changes in various metabolic pathways and their fluxes (including glucose

uptake, cytosolic glycolysis, mitochondrial Krebs cycle, energy metabolism, amino acids, ketone bodies and phospholipids precursors) are depicted in the metabolic array on Figure 4. No prominent changes in cell metabolism were observed in the bel-treated cells. In contrast, single-agent treatment with bor led to an initial inhibition of the mitochondrial Krebs cycle, a slight disturbance in energy metabolism (decreased phosphocreatine and total creatine) and decreased phospholipid turnover (decreased ratios of phosphocholine to glycerophosphocholine, [PCho/GPC]) after 24 h of treatment. However, all these metabolic disturbances returned to baseline by 48 h. The most prominent changes on bor treatment were related neither to glucose nor to phospholipid metabolism but to accumulation of intracellular amino acids and increased antioxidative cell defense at 24 h, which persisted at 48 h. Cellular stress induced by bor was also reflected in the increased concentration of cellular osmolytes. The combination treatment mimicked, in general, the metabolic signature of proteasome inhibition (accumulation of amino acids and increased oxidative stress). However, inhibition of mitochondrial glucose metabolism as well as cytosolic glycolysis was observed at 48 h, suggesting that the presence of bel abolished the compensatory mechanisms induced by single-agent bor exposure. The synergistic inhibition of cell proliferation after combination treatment was confirmed by highly decreased cell wet weights and reflected in the decreased cell mass concentrations of choline and phosphocholine (membrane phospholipid precursors) and decreased phospholipid turnover (decreased [PCho/GPC] ratios). Interestingly, no decrease in glucose uptake was observed in either treatment group.

Discussion

Despite ongoing efforts to develop new treatment strategies in PC and HCC, there has been limited success in implementing clinically meaningful novel chemotherapeutic therapies. This research group recently demonstrated synergistic inhibition of proliferation and induction of apoptosis and cell-cycle arrest in colorectal cancer cell lines *in vitro* with a combination of HDAC and proteasome inhibition (29). Based on those findings, this study focused on developing a similar rational combination treatment strategy for PC and HCC. It was hypothesized that the combination of bel, an HDAC inhibitor, and bor, a proteasome inhibitor, would result in synergistic antitumor activity against PC and HCC. The present study demonstrated inhibition of proliferation and induction of apoptosis *in vitro* in PC and HCC cell lines, as well as characteristic molecular and metabolic endpoints for HDAC and proteasome inhibition.

An emerging area of interest in oncology involves the role of epigenetics in the control of cancer development and progression. Specifically, understanding the role of the nucleosomes and the histone subunits, as well as modifications that regulate gene transcription, and their dysregulation in cancer is a novel area to exploit for anticancer therapy (30–33). Acetylation and deacetylation of histones occurs *via* HATs and HDACs, respectively, resulting in alterations in the structure of chromatin which, in turn, affects dynamic transcriptional expression of protooncogenes and tumor suppressor genes (10, 34). The most advanced class of anticancer agents in this area are the HDAC inhibitors. Vorinostat is the only approved HDAC inhibitor but multiple other compounds are currently under study, including bel (13). Inhibiting the proteasome has also proven fruitful as an anticancer management strategy. Bor, a dipeptide inhibitor of the 26S proteasome, is clinically indicated in multiple myeloma, and has also shown single-agent activity against xenograft models of melanoma, adult T-cell leukemia, lung, breast and prostate cancer (22, 35–40). Evidence also suggests bor potentiates the antitumor effects of chemotherapy (41–44).

This study evaluated the antiproliferative activity of the combination of HDAC and proteasome inhibition on PC and HCC cell lines and demonstrated that both bel and bor exert single-agent effects. Additionally, synergistic inhibition of proliferation was observed when these cell lines were exposed concurrently to the combination of bel and bor. Notably, the mechanisms by which HDAC and proteasome inhibitors exert their cytotoxic effects are not fully delineated, are likely to be multifactorial and have been proven to be cell line-specific; reports have included the increased expression of the cell-cycle regulators p21 and p27 for both HDAC and proteasome inhibitors, as well as the destruction of intracellular signaling proteins including p53, the inhibitor of NFκB (IκB), and antiapoptotic proteins, in the case of proteasome inhibition (45–48). The present data corroborates previously published data describing bel-induced suppression of cancer cell growth *in vitro* and *in vivo* in bladder, prostate, ovarian and colon cancer models (49–52). Across these studies, single-agent low micromolar IC_{50} values were attained *in vitro* with bladder cancer cell lines exhibiting the highest IC_{50} at 10 μM (49). With regard to single-agent bor, IC_{50} values obtained in the present study paralleled those observed from other studies (53, 54). Interestingly, despite the relatively resistant phenotypes of PC and HCC, the cell lines tested in this study achieved similar IC_{50} values with both agents. As expected, PC and HCC cell lines sustained up-regulation of p21, particularly at the higher single-agent exposures and with the combination bel+bor, suggesting that cell-cycle inhibition is potentiated with combined inhibition.

Previous studies have demonstrated anti-proliferative synergy of HDAC and proteasome inhibitors in combination, two of them examining bel and bor, in multiple myeloma and chronic lymphocytic leukemia (55–58). These studies reported that growth inhibition is associated with induction of apoptosis with increases and decreases in pro- (Bim) and anti-apoptotic (Bcl-xL, Mcl-1, XIAP) proteins, respectively, and the generation of reactive oxygen species mediating DNA damage (55, 56). To investigate whether the inhibition of proliferation in PC and HCC cell lines in this study was due to a cytostatic effect or an increase in apoptosis, the study determined the activity of caspase−3/−7, well-recognized markers of the execution phase of apoptosis, and demonstrated that not only was apoptosis increased with exposure to the single agents, but strikingly induced by the combination. Interestingly, the assessment of apoptosis using a caspase−3/−7 assay demonstrated early induction after only 12 h of drug exposure, implying apoptosis induction occurs rapidly with combined HDAC and proteasome inhibition. In addition, although the confirmatory apoptotic assay of PARP cleavage was consistent with the caspase assay results in BxPC3 cells, PARP cleavage in the Hep1 cells, although present, was not as extensive. Although not completely understood, others have also found a disassociation between caspase−3/−7 activity and PARP cleavage, possibly implicating other effector enzymes, such as caspase-2, −6 and −9, as major propagators of the apoptotic cascade in cell lines that exhibit relative resistance (59, 60).

In this study, aH3 expression was used as a means of confirming target inhibition with the HDAC inhibitor. As expected, acetylation of H3 was observed in both histological tumor subtypes, when exposed to bel that persisted for at least 24 h. Additionally, in Hep1 but not BxPC3 cells, H3 was also acetylated in cells after exposure to single-agent bor. Although not previously described with proteasome inhibition, HCC has been shown to have aberrant histone modifications with the suggestion that a higher level of acetylated H3 is a negative prognostic feature (61, 62). Interestingly, in both PC and HCC cell lines, p-NFκB was up-regulated, particularly with high-dose bor and all bel+bor combinations. NFκB, thought to be blocked by proteasome inhibitors, is a transcription factor regulating genes involved in proliferation, apoptosis and angiogenesis and is particularly well-studied as the main effector of apoptosis in multiple myeloma (20). NFκB is known to be overexpressed or constitutively active in a number of human tumor types, possibly conferring resistance to

cancer cell death (63, 64). The observation that NFκB is up-regulated with HDAC and proteasome inhibition is contrary to most previously published work but is not unprecedented with an increase in NFκB transcription, observed with proteasome inhibition in endometrial carcinoma cell explants, while still inducing cell death (65). These data suggest the need for re-evaluation of the role of NFκB as it pertains to apoptosis in particular tumor types and possibly suggests an alternative pathway for apoptosis induction in PC and HCC cell lines.

Lastly, establishing metabolic signatures for signal transduction inhibitors is an emerging area in preclinical and clinical assessment of therapy response (66, 67). Indeed, *in vitro* and *in vivo* cytostatic effects of several tyrosine kinase inhibitors (including Bcr-Abl, EGFR and Akt-pathway modulators) are mostly attributed to significant decreases in glucose uptake and metabolism, as revealed by this research group as well as others (27, 66, 68). Importantly, metabolic endpoints of therapeutic response can later be translated into noninvasive clinical protocols using metabolic imaging modalities such as positron-emission tomography or magnetic resonance spectroscopy. Currently, there are no existing reports on the metabolic signatures attributed to the inhibition of HDAC or proteasome pathways. This study, for the first time, reported that HDAC inhibition results in no appreciable metabolic consequences in PC and HCC cell lines. Proteasome inhibition also failed to modulate glucose uptake and metabolism in the cells; however, it resulted in characteristic changes (accumulation) in amino acid and cellular antioxidants. This metabolic signature of bor treatment supports previous findings by other groups which demonstrated disturbances in protein degradation and stress response. Although bel alone did not prove to be a metabolic modulator, it enhanced the metabolic aberrations of proteasome inhibition, which resulted in highly increased levels of amino acids and antioxidative defense mechanisms. The cytotoxic nature of the bel and bor combination also resulted in nonspecific decreases in glucose metabolism at 48 h, while their synergistic inhibition of cell proliferation was reflected in a slightly decreased membrane phospholipid turnover.

In summary, the preclinical data from this study suggest that a combination therapy with bel and bor warrants further investigation in HCC and PC models. The study indicated significant synergy in both inhibition of proliferation and induction of apoptosis with the use of bel in combination with bor in multiple HCC and PC cell lines *in vitro*. Such strategies that incorporate dual novel agents, without standard cytotoxics, may be warranted in diseases such as HCC and PC where chemotherapy has limited efficacy and combinations have not led to breakthroughs in clinical benefit. Such studies should build upon preclinical data reported here and elsewhere by incorporating relevant biomarkers to further elucidate mechanisms of activity and, likewise, of resistance. The *in vitro* established metabolic endpoints presented here should also be considered in the design of subsequent *in vivo* preclinical and clinical studies.

Acknowledgments

The primary author would like to recognize the mentorship she received from her co-authors and thank the National Cancer Institute of Canada, the Terry Fox Foundation, and the Alberta Heritage Foundation for Medical Research for grant support of her fellowship at the University of Colorado.

References

1. Jemal A, Siegel R, Ward E, Hao Y, Xu J, Thun MJ. Cancer statistics, 2009. CA Cancer J Clin. 2009; 59:225–249. [PubMed: 19474385]
2. Burris HA 3rd, Moore MJ, Andersen J, Green MR, Rothenberg ML, Modiano MR, Cripps MC, Portenoy RK, Storniolo AM, Tarassoff P, Nelson R, Dorr FA, Stephens CD, Von Hoff DD. Improvements in survival clinical benefit with gemcitabine as first-line therapy for patients with

advanced pancreas cancer a randomized trial. J Clin Oncol. 1997; 15:2403–2413. [PubMed: 9196156]

3. Moore MJ, Goldstein D, Hamm J, Figer A, Hecht JR, Gallinger S, Au HJ, Murawa P, Walde D, Wolff RA, Campos D, Lim R, Ding K, Clark G, Voskoglou-Nomikos T, Ptasynski M, Parulekar W. Erlotinib plus gemcitabine compared with gemcitabine alone in patients with advanced pancreatic cancer a phase III trial of the National Cancer Institute of Canada Clinical Trials Group. J Clin Oncol. 2007; 25:1960–1966. [PubMed: 17452677]
4. Llovet JM, Ricci S, Mazzaferro V, Hilgard P, Gane E, Blanc JF, de Oliveira AC, Santoro A, Raoul JL, Forner A, Schwartz M, Porta C, Zeuzem S, Bolondi L, Greten TF, Galle PR, Seitz JF, Borbath I, Haussinger D, Giannaris T, Shan M, Moscovici M, Voliotis D, Bruix J. Sorafenib in advanced hepatocellular carcinoma. N Engl J Med. 2008; 359:378–390. [PubMed: 18650514]
5. Monneret C. Histone deacetylase inhibitors for epigenetic therapy of cancer. Anticancer Drugs. 2007; 18:363–370. [PubMed: 17351388]
6. Mehnert JM, Kelly WK. Histone deacetylase inhibitors biology and mechanism of action. Cancer J. 2007; 13:23–29. [PubMed: 17464243]
7. Marks PA, Richon VM, Breslow R, Rifkind RA. Histone deacetylase inhibitors as new cancer drugs. Curr Opin Oncol. 2001; 13:477–483. [PubMed: 11673688]
8. Wang J, Saunthararajah Y, Redner RL, Liu JM. Inhibitors of histone deacetylase relieve ETO-mediated repression and induce differentiation of AML1-ETO leukemia cells. Cancer Res. 1999; 59:2766–2769. [PubMed: 10383127]
9. Borrow J, Stanton VP Jr, Andresen JM, Becher R, Behm FG, Chaganti RS, Civin CI, Disteche C, Dube I, Frischauf AM, Horsman D, Mitelman F, Volinia S, Watmore AE, Housman DE. The translocation t(8;16)(p11;pl3) of acute myeloid leukaemia fuses a putative acetyltransferase to the CREB-binding protein. Nat Genet. 1996; 14:33–41. [PubMed: 8782817]
10. Johnstone RW. Histone-deacetylase inhibitors novel drugs for the treatment of cancer. Nat Rev Drug Discov. 2002; 1:287–299. [PubMed: 12120280]
11. Xu WS, Parmigiani RB, Marks PA. Histone deacetylase inhibitors molecular mechanisms of action. Oncogene. 2007; 26:5541–5552. [PubMed: 17694093]
12. Mann BS, Johnson JR, Cohen MH, Justice R, Pazdur R. FDA approval summary vorinostat for treatment of advanced primary cutaneous T-cell lymphoma. Oncologist. 2007; 12:1247–1252. [PubMed: 17962618]
13. Glaser KB. HDAC inhibitors clinical update and mechanism-based potential. Biochem Pharmacol. 2007; 74:659–671. [PubMed: 17498667]
14. Odenike O, Green M, Larson R, Rich E, Ott J, Ratain M, Stock W. Phase I study of belinostat (PXD101) plus azacitidine (AZC) in patients with advanced myeloid neoplasms. J Clin Oncol. 2008; 26
15. Mackay H, Hirte HW, Covens A, Mac Alpine K, Wang L, Tsao MS, Pan J, Zwiebel JA, Oza AM. A phase II trial of the histone deacetylase inhibitor belinostat (PXD101) in patients with platinum resistant epithelial ovarian tumors and micropapillary/borderline (LMP) ovarian tumors. A PMH phase II consortium trial. J Clin Oncol. 2008; 26
16. Kelly WK, Yap T, Lee J, Lassen U, Crowley E, Clarke A, Hawthorne T, Buhl-Jensen P, Bono JD. A phase I study of oral belinostat (PXD101) in patients with advanced solid tumors. J Clin Oncol. 2007; 25:14092.
17. Yeo W, Lim R, MA BB, Hui P, Chan L, Mo FK, Yu SC, Ho SS, Koh J, Chan AT, Goh B. A phase I/II study of belinostat (PXD101) in patients with unresectable hepatocellular carcinoma. J Clinical Oncol. 2007; 25:15081.
18. Sinha R, Moliffe R, Scurr M, Vidal L, Engelholm SA, Jensen PB, Normann A, Li S, Bono JD, Lassen U. A phase I/II study of the safety and anticancer activity of IV-administered belinostat (PXD101) plus carboplatin (C) or paclitaxel (P), or both in patients with advanced solid tumors. J Clinical Oncol. 2007; 25:3574.
19. O'Bryant, C.; Leong, S.; Camidge, D.; Gore, L.; Diab, S.; Call, J.; Spratlin, J.; Zwiebel, J.; Eckhardt, SG. A phase 1 study of belinostat (PXD101) in combination with bortezomib in patients with advanced solid tumors and lymphoma; Proceedings of Annual AACR Meeting, San Francisco; California. 2007.

20. Milano A, Iaffaioli RV, Caponigro F. The proteasome: a worthwhile target for the treatment of solid tumours? Eur J Cancer. 2007; 43:1125–1133. [PubMed: 17379504]
21. Landis-Piwowar KR, Milacic V, Chen D, Yang H, Zhao Y, Chan TH, Yan B, Dou QP. The proteasome as a potential target for novel anticancer drugs and chemosensitizers. Drug Resist Updat. 2006; 9:263–273. [PubMed: 17197231]
22. Boccadoro M, Morgan G, Cavenagh J. Preclinical evaluation of the proteasome inhibitor bortezomib in cancer therapy. Cancer Cell Int. 2005; 5:18. [PubMed: 15929791]
23. Papazisis KT, Geromichalos GD, Dimitriadis KA, Kortsaris AH. Optimization of the sulforhodamine B colorimetric assay. J Immunol Methods. 1997; 208:151–158. [PubMed: 9433470]
24. Chou TC, Talalay P. Analysis of combined drug effects A new look at a very old problem. Trends Pharmacol Sci. 1983; 4:450–454.
25. Serkova NJ, Glunde K. Metabolomics of cancer. Methods Mol Biol. 2009; 520:273–295. [PubMed: 19381962]
26. Kominsky DJ, Klawitter J, Brown JL, Boros LG, Melo JV, Eckhardt SG, Serkova NJ. Abnormalities in glucose uptake and metabolism in imatinib-resistant human BCR-ABL-positive cells. Clin Cancer Res. 2009; 15:3442–3450. [PubMed: 19401345]
27. Klawitter J, Kominsky DJ, Brown JL, Klawitter J, Christians U, Leibfritz D, Melo JV, Eckhardt SG, Serkova NJ. Metabolic characteristics of imatinib resistance in chronic myeloid leukaemia cells. Br J Pharmacol. 2009; 158:588–600. [PubMed: 19663881]
28. Serkova NJ, Christians U, Benet LZ. Biochemical mechanisms of cyclosporine neurotoxicity. Mol Interv. 2004; 4:97–107. [PubMed: 15087483]
29. Pitts TM, Morrow M, Kaufman SA, Tentler JJ, Eckhardt SG. Vorinostat and bortezomib exert synergistic antiproliferative and proapoptotic effects in colon cancer cell models. Mol Cancer Ther. 2009; 8:342–349. [PubMed: 19174560]
30. Villar-Garea A, Esteller M. Histone deacetylase inhibitors understanding a new wave of anticancer agents. Int J Cancer. 2004; 112:171–178. [PubMed: 15352027]
31. Dokmanovic M, Marks PA. Prospects histone deacetylase inhibitors. J Cell Biochem. 2005; 96:293–304. [PubMed: 16088937]
32. Lin HY, Chen CS, Lin SP, Weng JR, Chen CS. Targeting histone deacetylase in cancer therapy. Med Res Rev. 2006; 26:397–413. [PubMed: 16450343]
33. Liu T, Kuljaca S, Tee A, Marshall GM. Histone deacetylase inhibitors multifunctional anticancer agents. Cancer Treat Rev. 2006; 32:157–165. [PubMed: 16516391]
34. Marks PA, Richon VM, Kelly WK, Chiao JH, Miller T. Histone deacetylase inhibitors development as cancer therapy. Novartis Found Symp. 2004; 259:269–281. discussion 281–268. [PubMed: 15171260]
35. Amiri KI, Horton LW, LaFleur BJ, Sosman JA, Richmond A. Augmenting chemosensitivity of malignant melanoma tumors *via* proteasome inhibition implication for bortezomib (VELCADE, PS-341) as a therapeutic agent for malignant melanoma. Cancer Res. 2004; 64:4912–4918. [PubMed: 15256463]
36. Teicher BA, Ara G, Herbst R, Palombella VJ, Adams J. The proteasome inhibitor PS-341 in cancer therapy. Clin Cancer Res. 1999; 5:2638–2645. [PubMed: 10499643]
37. Williams S, Pettaway C, Song R, Papandreou C, Logothetis C, McConkey DJ. Differential effects of the proteasome inhibitor bortezomib on apoptosis and angiogenesis in human prostate tumor xenografts. Mol Cancer Ther. 2003; 2:835–843. [PubMed: 14555702]
38. Adams J, Palombella VJ, Sausville EA, Johnson J, Destree A, Lazarus DD, Maas J, Pien CS, Prakash S, Elliott PJ. Proteasom einhibitors a novel class of potent and effective antitumor agents. Cancer Res. 1999; 59:2615–2622. [PubMed: 10363983]
39. Satou Y, Nosaka K, Koya Y, Yasunaga JI, Toyokuni S, Matsuoka M. Proteasome inhibitor, bortezomib, potently inhibits the growth of adult T-cell leukemia cells both *in vivo* and *in vitro* . Leukemia. 2004; 18:1357–1363. [PubMed: 15190257]
40. Tan C, Waldmann TA. Proteasome inhibitor PS-341, a potential therapeutic agent for adult T-cell leukemia. Cancer Res. 2002; 62:1083–1086. [PubMed: 11861386]

41. Cusack JC Jr, Liu R, Houston M, Abendroth K, Elliott PJ, Adams J, Baldwin AS Jr. Enhanced chemosensitivity to CPT-11 with proteasome inhibitor PS-341 implications for systemic nuclear factor-kappaB inhibition. Cancer Res. 2001; 61:3535–3540. [PubMed: 11325813]
42. Bae SH, Ryoo HM, Kim MK, Lee KH, Sin JI, Hyun MS. Effects of the proteasome inhibitor bortezomib alone and in combination with chemotherapeutic agents in gastric cancer cell lines. Oncol Rep. 2008; 19:1027–1032. [PubMed: 18357392]
43. Wagenblast J, Hambek M, Baghi M, Gstottner W, Strebhardt K, Ackermann H, Knecht R. Antiproliferative activity of bortezomib alone and in combination with cisplatin or docetaxel in head and neck squamous cell carcinoma cell lines. J Cancer Res Clin Oncol. 2008; 134:323–330. [PubMed: 17701215]
44. Jung CS, Zhou Z, Khuri FR, Sun SY. Assessment of apoptosis-inducing effects of docetaxel combined with the proteasome inhibitor PS-341 in human lung cancer cells. Cancer Biol Ther. 2007; 6:749–754. [PubMed: 17387269]
45. Glaser KB, Staver MJ, Waring JF, Stender J, Ulrich RG, Davidsen SK. Gene expression profiling of multiple histone deacetylase (HDAC) inhibitors defining a common gene set produced by HDAC inhibition in T24 and MDA carcinoma cell lines. Mol Cancer Ther. 2003; 2:151–163. [PubMed: 12589032]
46. Yin D, Ong JM, Hu J, Desmond JC, Kawamata N, Konda BM, Black KL, Koeffler HP. Suberoylanilide hydroxamic acid a histone deacetylase inhibitor effects on gene expression and growth of glioma cells *in vitro* and *in vivo* . Clin Cancer Res. 2007; 13:1045–1052. [PubMed: 17289901]
47. Kumagai T, Wakimoto N, Yin D, Gery S, Kawamata N, Takai N, Komatsu N, Chumakov A, Imai Y, Koeffler HP. Histone deacetylase inhibitor, suberoylanilide hydroxamic acid (Vorinostat, SAHA) profoundly inhibits the growth of human pancreatic cancer cells. Int J Cancer. 2007; 121:656–665. [PubMed: 17417771]
48. Rajkumar SV, Richardson PG, Hideshima T, Anderson KC. Proteasome inhibition as a novel therapeutic target in human cancer. J Clin Oncol. 2005; 23:630–639. [PubMed: 15659509]
49. Buckley MT, Yoon J, Yee H, Chiriboga L, Liebes L, Ara G, Qian X, Bajorin DF, Sun TT, Wu XR, Osman I. The histone deacetylase inhibitor belinostat (PXD101) suppresses bladder cancer cell growth *in vitro* and *in vivo* . J Transl Med. 2007; 5:49. [PubMed: 17935615]
50. Qian X, Ara G, Mills E, LaRochelle WJ, Lichenstein HS, Jeffers M. Activity of the histone deacetylase inhibitor belinostat (PXD101) in preclinical models of prostate cancer. Int J Cancer. 2008; 122:1400–1410. [PubMed: 18027850]
51. Plumb JA, Finn PW, Williams RJ, Bandara MJ, Romero MR, Watkins CJ, La Thangue NB, Brown R. Pharmacodynamic response and inhibition of growth of human tumor xenografts by the novel histone deacetylase inhibitor PXD101. Mol Cancer Ther. 2003; 2:721–728. [PubMed: 12939461]
52. Qian X, LaRochelle WJ, Ara G, Wu F, Petersen KD, Thougaard A, Sehested M, Lichenstein HS, Jeffers M. Activity of PXD101, a histone deacetylase inhibitor in preclinical ovarian cancer studies. Mol Cancer Ther. 2006; 5:2086–2095. [PubMed: 16928830]
53. Colado E, Alvarez-Fernandez S, Maiso P, Martin-Sanchez J, Vidriales MB, Garayoa M, Ocio EM, Montero JC, Pandiella A, San Miguel JF. The effect of the proteasome inhibitor bortezomib on acute myeloid leukemia cells and drug resistance associated with the CD34+ immature phenotype. Haematologica. 2008; 93:57–66. [PubMed: 18166786]
54. Servida F, Soligo D, Delia D, Henderson C, Brancolini C, Lombardi L, Deliliers GL. Sensitivity of human multiple myelomas and myeloid leukemias to the proteasome inhibitor I. Leukemia. 2005; 19:2324–2331. [PubMed: 16224484]
55. Dai Y, Chen S, Kramer LB, Funk VL, Dent P, Grant S. Interactions between bortezomib and romidepsin and belinostat in chronic lymphocytic leukemia cells. Clin Cancer Res. 2008; 14:549–558. [PubMed: 18223231]
56. Feng R, Oton A, Mapara MY, Anderson G, Belani C, Lentzsch S. The histone deacetylase inhibitor, PXD101, potentiates bortezomib-induced anti-multiple myeloma effect by induction of oxidative stress and DNA damage. Br J Haematol. 2007; 139:385–397. [PubMed: 17910628]
57. Heider U, von Metzler I, Kaiser M, Rosche M, Sterz J, Rotzer S, Rademacher J, Jakob C, Fleissner C, Kuckelkorn U, Kloetzel PM, Sezer O. Synergistic interaction of the histone deacetylase

inhibitor SAHA with the proteasome inhibitor bortezomib in mantle cell lymphoma. Eur J Haematol. 2008; 80:133–142. [PubMed: 18005386]

58. Baradari V, Hopfner M, Huether A, Schuppan D, Scherubl H. Histone deacetylase inhibitor MS-275 alone or combined with bortezomib or sorafenib exhibits strong antiproliferative action in human cholangiocarcinoma cells. World J Gastroenterol. 2007; 13:4458–4466. [PubMed: 17724801]
59. Del Bello B, Valentini MA, Mangiavacchi P, Comporti M, Maellaro E. Role of caspases-3 and −7 in Apaf-1 proteolytic cleavage and degradation events during cisplatin-induced apoptosis in melanoma cells. Exp Cell Res. 2004; 293:302–310. [PubMed: 14729468]
60. Janicke RU, Ng P, Sprengart ML, Porter AG. Caspase-3 is required for alpha-fodrin cleavage but dispensable for cleavage of other death substrates in apoptosis. J Biol Chem. 1998; 273:15540–15545. [PubMed: 9624143]
61. Lee JS, Chu IS, Heo J, Calvisi DF, Sun Z, Roskams T, Durnez A, Demetris AJ, Thorgeirsson SS. Classification and prediction of survival in hepatocellular carcinoma by gene expression profiling. Hepatology. 2004; 40:667–676. [PubMed: 15349906]
62. Tischoff I, Tannapfe A. DNA methylation in hepatocellular carcinoma. World J Gastroenterol. 2008; 14:1741–1748. [PubMed: 18350605]
63. Tai DI, Tsai SL, Chang YH, Huang SN, Chen TC, Chang KS, Liaw YF. Constitutive activation of nuclear factor kappaB in hepatocellular carcinoma. Cancer. 2000; 89:2274–2281. [PubMed: 11147598]
64. Rayet B, Gelinas C. Aberrant REL/NFκB genes and activity in human cancer. Oncogene. 1999; 18:6938–6947. [PubMed: 10602468]
65. Dolcet X, Llobet D, Encinas M, Pallares J, Cabero A, Schoenenberger JA, Comella JX, Matias-Guiu X. Proteasome inhibitors induce death but activate NF-kappaB on endometrial carcinoma cell lines and primary culture explants. J Biol Chem. 2006; 281:22118–22130. [PubMed: 16735506]
66. Spratlin JL, Serkova NJ, Eckhardt SG. Clinical applications of metabolomics in oncology a review. Clin Cancer Res. 2009; 15:431–440. [PubMed: 19147747]
67. Serkova NJ, Spratlin JL, Eckhardt SG. NMR-based metabolomics translational application and treatment of cancer. Curr Opin Mol Ther. 2007; 9:572–585. [PubMed: 18041668]
68. Marin S, Lee WN, Bassilian S, Lim S, Boros LG, Centelles JJ, FernAndez-Novell JM, Guinovart JJ, Cascante M. Dynamic profiling of the glucose metabolic network in fasted rat hepatocytes using [l,2–13C2]glucose. Biochem J. 2004; 381:287–294. [PubMed: 15032751]

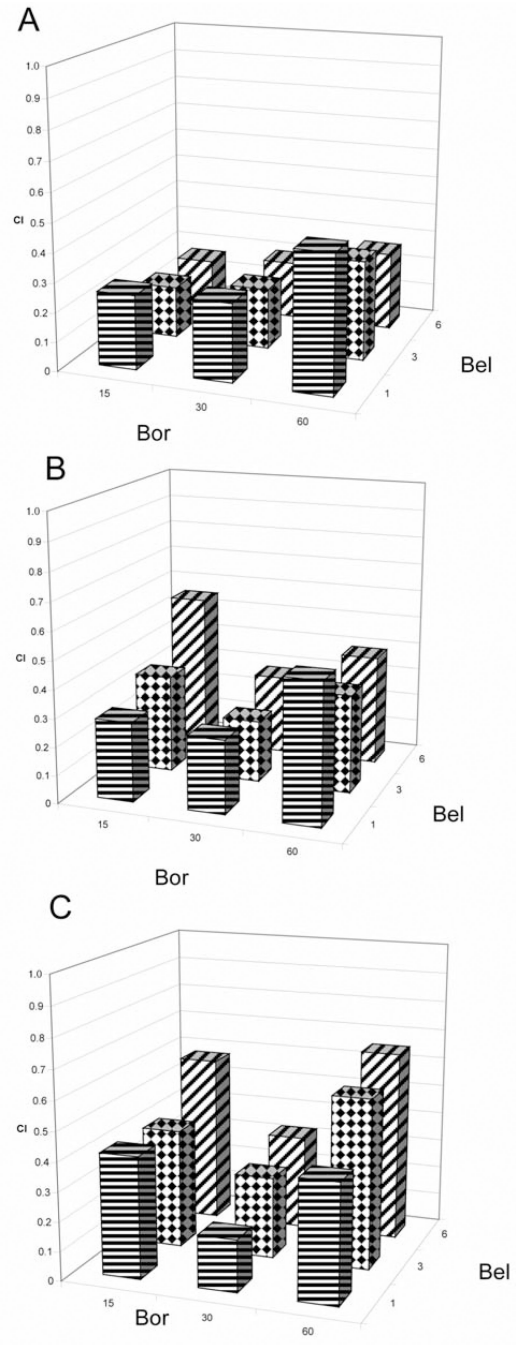

Figure 1.
Synergistic inhibition of proliferation when combining belinostat (bel) μM and bortezomib (bor) nM at A) 24-, B) 48-, and C) 72-hour exposure in Panel cells.

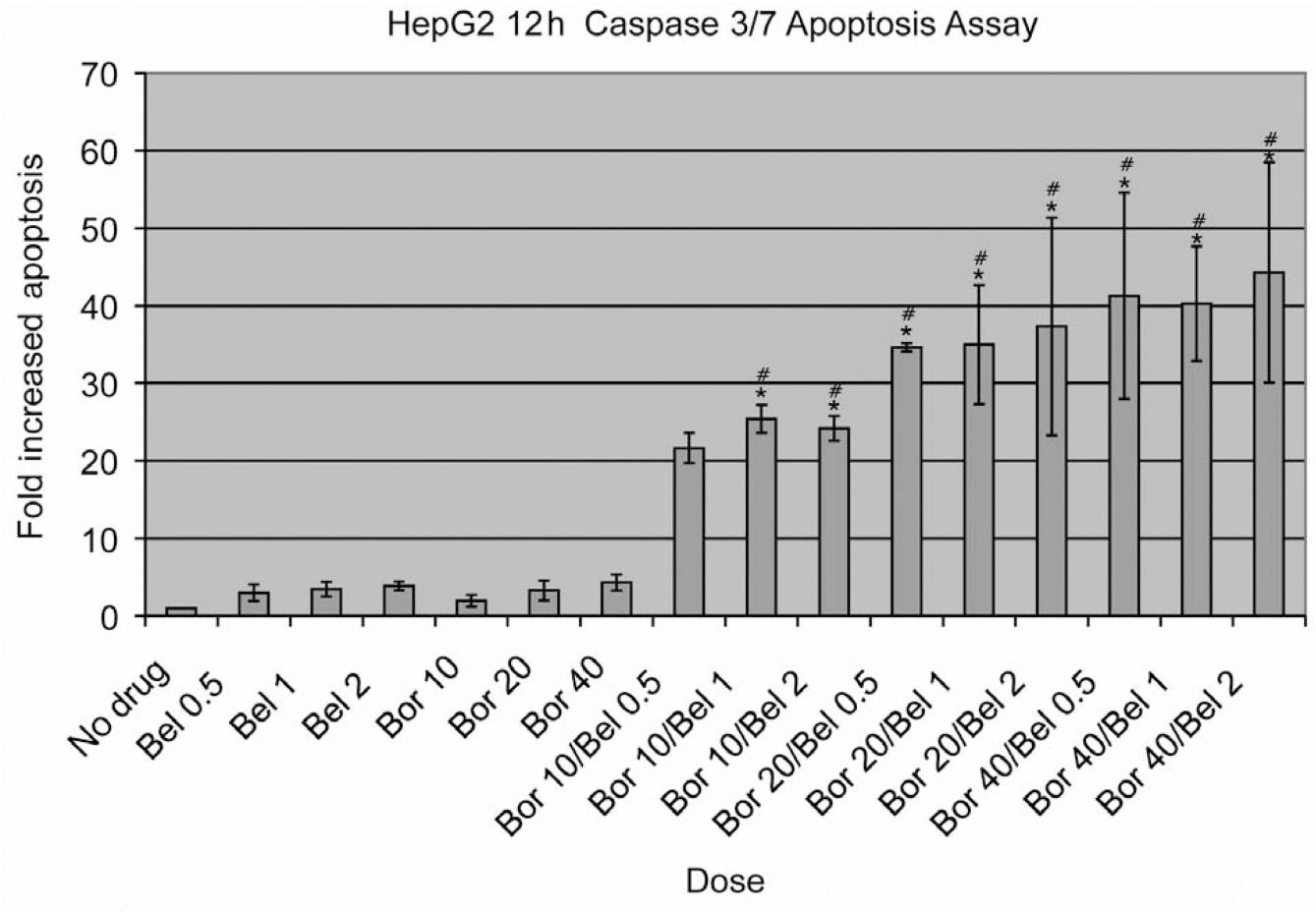

Figure 2.
HepG2 12-h apoptosis caspase-31-7 assay. Data are presented as mean±standard deviation of four replications. Doses of belinostat (bel) and bortezomib (bor) are expressed in μM and nM, respectively. *$p<0.05$ relative to single-agent Bel; $^{\#}p<0.05$ relative to single-agent Bor.

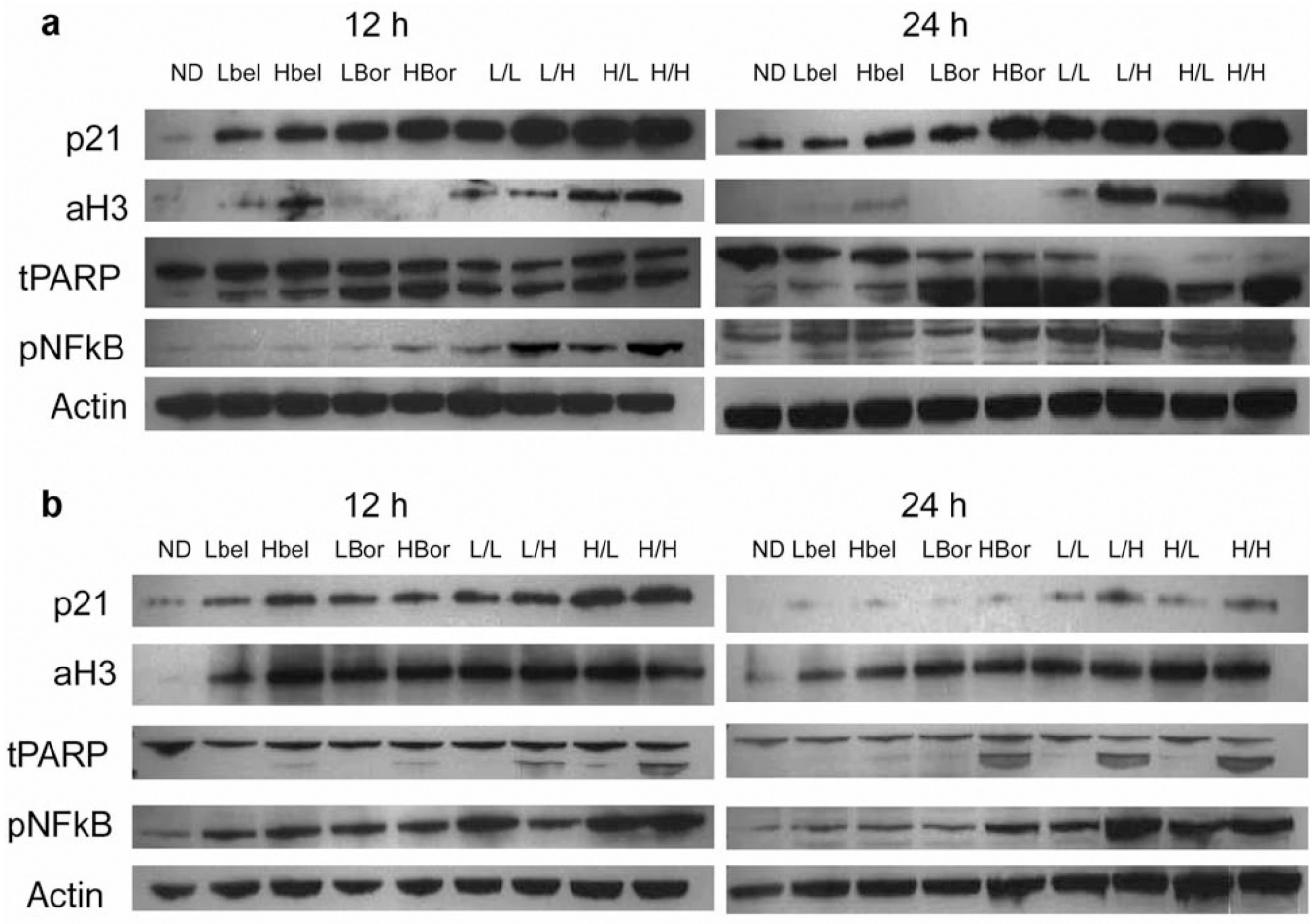

Figure 3.
Immunoblots of p21, aH3, tPARP, and p-NFκB, at 12 and 24 h post-treatment for (A) BxPC3 and (B) Hep1 cell lines. ND, No drug; bel, belinostat; bor, bortezomib; L, low-dose; H, high-dose; I, bellbor combination at the indicated doses.

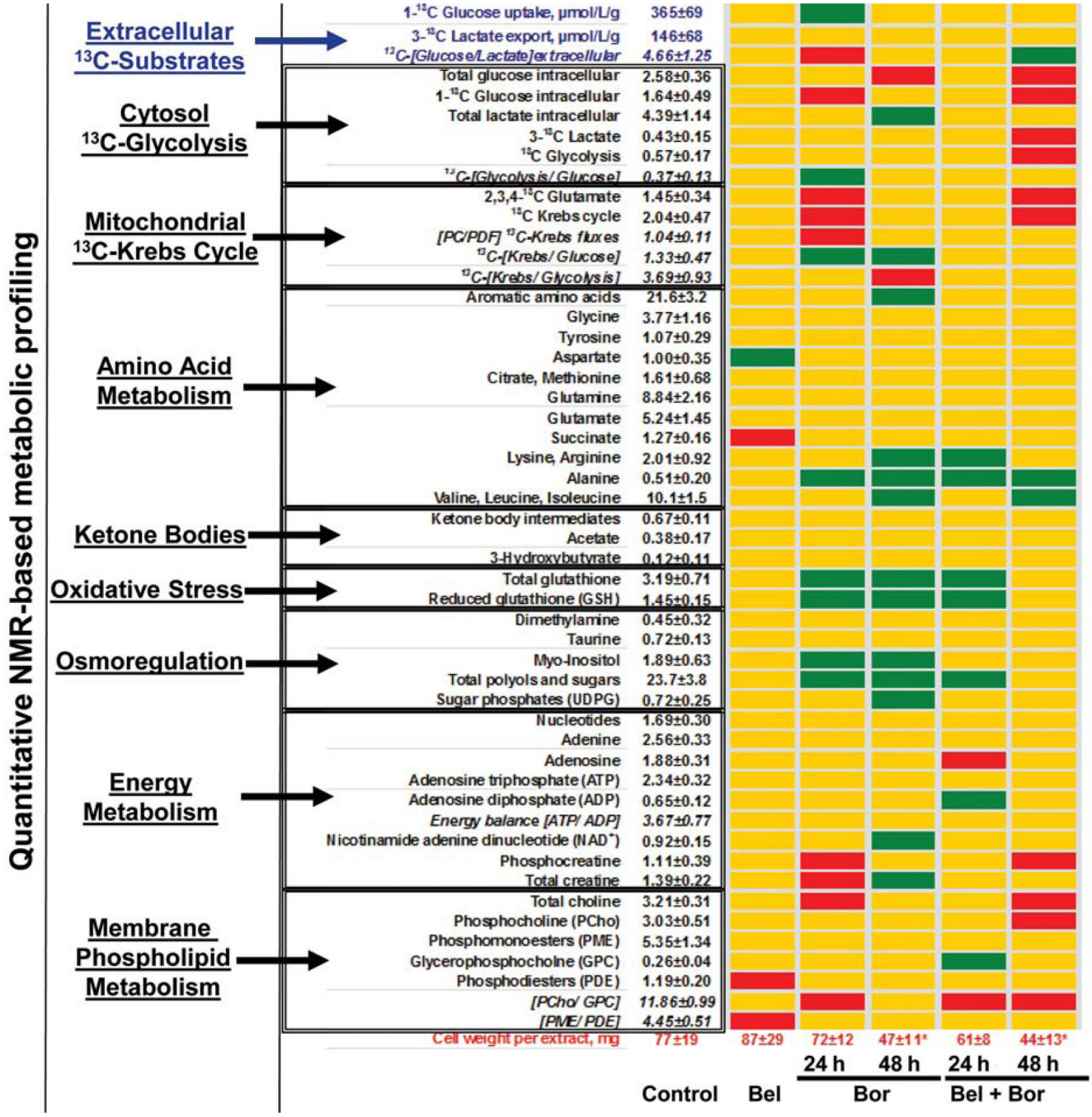

Figure 4.

Metabolic profile array established from quantitative metabolic NMR profiles from BxPC3 cell and media extracts. The metabolites, their ratios and metabolic fluxes were grouped based on their biochemical relevance. For the control group, all intracellular metabolite levels are given as µmol/cell wet weights; glucose uptake and lactate export are given as µmol/l/g cell weights. Metabolic pathways which were undisturbed by treatment are presented as yellow maps. A decrease in metabolic endpoint is indicated by red, while an increase is indicated by green spots. Statistical significance for cell weights (given in mg): *p<0.02. The metabolic profile array database was adapted from the interactive SIDMAParrayTM (68), available at http://www.sidmap.com.

Table I

Single agent IC_{50} values for belinostat (μm) and bortezomib (nM) exposure.

	Exposure time (hours)					
	24		48		72	
Cell line	Bel	Bor	Bel	Bor	Bel	Bor
BxPC3	---	100	4	25	1	25
Panc1	---	---	8	50	3	25
Hep1	---	50	4	25	0.5	25
HepG2	----	---	1	25	1	37.5